# Influence of Pedestrian Traffic on Capacity of Right-Turning Movements at Signalized Intersections

Xiao-ming Chen, Chun-fu Shao, and Yue Hao

**Pedestrians have a significant influence on vehicle capacities of turning movements at signalized intersections. The increasing emphasis on pedestrian traffic has highlighted deficiencies in the relevant research in China. It is imperative to quantify accurately the effect of pedestrians on vehicle capacity to provide a basis for traffic operations and facility designs in mixed traffic conditions. This study proposes an analytical model for the capacity of right-turning movements influenced by pedestrians at signalized intersections. The model takes into account pedestrian behavior, pedestrian–vehicle conflict mechanisms, and pedestrian arrivals in platoons. The conflict-zone capacity is modeled on the basis of the conflict mechanism. The model was calibrated and used as the basis to calculate right-turn vehicle capacities. The capacities yielded by the proposed model depend strongly on the average conflict times. The results show that pedestrians have a strong impact on the right-turn capacities at low pedestrian volumes and that the effects of additional pedestrians decrease as the pedestrian volumes increase. VISSIM was employed to simulate the interactions between right turns and pedestrians to validate the model. A numerical example is presented to compare the proposed model with the simulations and several existing analytical models. At low pedestrian volumes, the predictions of the other methods are approximately equal; at high pedestrian volumes, the models assuming pedestrian priority yield lower capacities than those assuming no priority.**

Increasing importance has been attached to pedestrian traffic as a healthy, sustainable alternative to automobile transportation. However, pedestrians have a significant effect on vehicle flow in mixed traffic conditions. The effect includes increased delays and decreased capacities as well as potential threats to road safety. As the bottlenecks of urban roads, intersections tend to be influenced more severely. Therefore, it is necessary to accurately quantify the influence of pedestrians on the turning-movement capacities of signalized intersections so as to provide a basis for facility designs and traffic operations.

## LITERATURE REVIEW

The reviewed literature contains various models to predict the effect of pedestrians on the vehicle capacity of signalized intersections. The existing analytical models that deal with the problem can be categorized into adjustment factor methods and gap-acceptance-based methods.

### Adjustment Factor Methods

Methods based on pedestrian adjustment factors are widely accepted and used to calculate the capacities of signalized intersections influenced by pedestrian traffic. Various procedures have been developed to estimate the adjustment factors. Among them, the most prevailing calculation procedure is the one proposed by the *Highway Capacity Manual* (HCM) (*1*). The HCM method describes the interactions of turning vehicles and pedestrians by using a conflict-zone-occupancy approach. It estimates the average pedestrian and bicycle occupancy at the conflict zone and then determines the relevant occupancy, which combines the effects of both pedestrians and bicycles. The adjustment factor can then be computed to calculate the saturation flow rate and capacity (*2, 3*). Rouphail and Eads (*4*) derived a regression model of the adjustment factor based on field data collected for an FHWA research project at North Carolina State University.

### Gap-Acceptance–Based Methods

Gap-acceptance–based methods have also been proposed. Viney and Pretty (*5*) presented a model to calculate the saturation flow rate when vehicles are required to give way to two-way pedestrian flow. The green phase is divided into five intervals. In the first and third intervals, pedestrian platoons block the vehicles, with no vehicle crossing. In the second and fourth intervals, vehicles accept gaps in the pedestrian flow. In the fifth interval, the pedestrian flow ceases and vehicles cross at the saturation flow rate. The capacity is then calculated.

### Simulation Methods

Besides analytical models, simulations have also been used to model the interactions between pedestrians and vehicles. Rouphail and Eads (*4*) used CORSIM to simulate the effects of pedestrians on right-turn saturation flow rates at signalized intersections. The simulated results were compared with several analytical methods.

## OBJECTIVES

These research achievements, particularly the HCM, provide deep insights and excellent resources to quantify the effects of pedestrians on capacities. However, pedestrians frequently are not just confined to the crosswalks when they cross at intersections in China, so the conflict zone is rather difficult to bound because of the uncertainties in its location. As a result, occupancy-based methods may have limited application because of the difficulties in data collection. The existing gap-acceptance-based models were developed assuming that pedestrians have priority over vehicles, which is not always true in China. In sum, these methods may not always be directly transferable to traffic engineering studies in China.

Therefore, the objectives of this research are (*a*) to propose an analytical model based on the pedestrian–vehicle conflict mechanism to quantify the effect of pedestrians on right-turn capacity when pedestrians have no strict priority over the right-turning traffic and (*b*) to compare the model with simulations and several existing analytical models.

## CONFLICT ZONE ANALYSIS

A conflict zone is a portion of an intersection, typically in the crosswalk, in which pedestrians and vehicles compete for space. Complex interactions occur between the competing pedestrians and vehicles at conflict zones in intersections.

Although pedestrian–vehicle conflicts can be avoided by time separation control, all the conflicts usually cannot be eliminated in consideration of traffic efficiency. Common conflicts between pedestrians and right turns are shown in Figure 1*a*. The conflict zones are usually the bottlenecks of the right-turning movements; therefore, the traffic conditions and conflict mechanisms serve as the basis for capacity calculations.

### Pedestrian Arrivals in Platoons

Pedestrians usually walk together in platoons on sidewalks or crosswalks, which is different from vehicles, which move one after another in lanes.

A pedestrian platoon is a group of pedestrians traveling together as a group, either voluntarily or involuntarily because of signal control, geometrics, or other factors (e.g., pedestrians who know each other) (*1*). In this study, two pedestrians are regarded as being in one pedestrian platoon if the headway between them is less than 1 s. The period of 1 s is selected because that headway is so short that vehicles cannot accept such a small gap to cross the pedestrian flow. Instead of an individual pedestrian, the pedestrian platoon is used as the basic unit to perform the gap-acceptance analysis for capacity calculation in the study.

As concluded by Huang and Yang (*6*), pedestrian platoon headways defined as such have a shifted-exponential distribution when the volume is lower than 4,000 ped/h. The cumulative distribution function of the pedestrian platoon headways can be written as

$$P(h_p \le t) = 1 - \exp\left(\frac{-(t-1)}{(H_p - 1)}\right) \tag{1}$$

where

$P$ = pedestrian flow,
$h_P$ = headway of the pedestrian platoons in seconds,
$t$ = independent variable of the distribution function in seconds, and
$H_P$ = mean headway of pedestrian platoons in seconds.

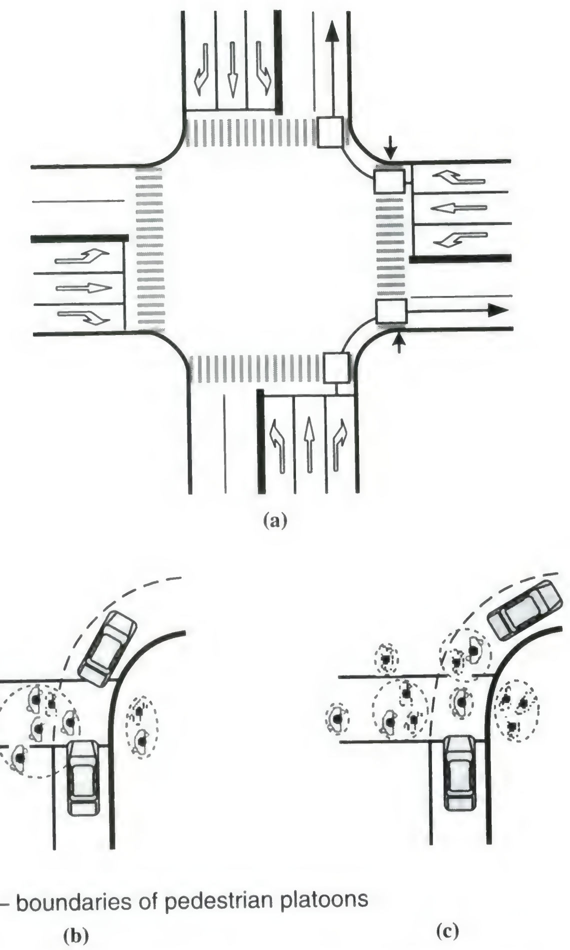


FIGURE 1 Common pedestrian and right-turn conflicts at typical signalized intersections: (*a*) conflict zones, (*b*) conflict with one-way pedestrian flow, and (*c*) conflict with two-way pedestrian flow.

Usually, mean platoon size increases as pedestrian volumes increase. Therefore, the mean platoon size should correlate with the pedestrian volume, which can be mathematically modeled by the following linear equation:

$$N = \alpha_0 + \alpha_1 \cdot p \qquad N \ge 1 \tag{2}$$

where

$N$ = mean platoon size in number of pedestrians,
$p$ = pedestrian volume in pedestrians per hour, and
$\alpha_0$ and $\alpha_1$ = regression coefficients.

The equation provides a measure of the extent of pedestrian arrivals in platoons.

The mean headway of the arriving pedestrian platoons is

$$H_p = 3{,}600 \cdot \frac{N}{p} = 3{,}600 \cdot \frac{(\alpha_0 + \alpha_1 \cdot p)}{p} \tag{3}$$

### Effect of Number of Waiting Pedestrians and Waiting Time

Usually pedestrians will have an increased sense of security and tend to behave with less prudence when more pedestrians are waiting at

School of Traffic and Transportation, Beijing Jiaotong University, Campus Post Office Box 617, Beijing 100044, China. Corresponding author: X. Chen, chenxm11@163.com.

*Transportation Research Record: Journal of the Transportation Research Board, No. 2073*, Transportation Research Board of the National Academies, Washington, D.C., 2008, pp. 114–124.
DOI: 10.3141/2073-13

the conflict zone. The individuals in the platoon tend to accept smaller gaps as the number of waiting pedestrians increases.

In addition, pedestrians usually become increasingly impatient and then tend to take risks and accept smaller gaps as their waiting time increases.

### Pedestrian–Vehicle Conflict Mechanism

According to the Chinese road safety laws, drivers should decelerate and yield when they encounter pedestrians in crosswalks. However, in China drivers are seldom ready to give way to pedestrians in intersections. When the right-of-way is allocated to pedestrians and vehicles simultaneously, neither of them has priority over the other at the conflict zone. As a result, pedestrians and vehicles alternately wait for acceptable gaps and cross the competing flow in platoons.

The vehicle flow or pedestrian flow occupying the conflict zone can be divided into a saturated flow at first and then an unsaturated flow. The saturated flow is delayed by the competing flow, and then the waiting units cross at the saturation flow rate when an acceptable gap occurs for them. The unsaturated flow does not incur delays but will be impeded when an acceptable gap for the competing flow occurs. This process repeats periodically as the vehicles interact with the pedestrians. This mechanism is adopted as a fundamental assumption of the conflict-zone capacity model.

## CONFLICT ZONE CAPACITY

To illustrate the capacity calculation procedure, the simple situation shown in Figure 1*b* is taken as an example.

The conflict cycle is defined as the period during which the right-turning vehicle flow, *V*, and the pedestrian flow, *P*, cross each other once at the conflict zone. The conflict cycle is denoted by *C*, in seconds. In the conflict cycle, the duration of vehicle flow is denoted by $T_{Vi}$ and that of the pedestrian flow by $T_P$. Thus, $C = T_{Vi} + T_P$.

The durations of the vehicle and pedestrian saturated flows are denoted by $T_{SV}$ and $T_{SP}$, respectively, with the corresponding mean number of passed vehicles and pedestrian platoons denoted by $N_{SV}$ and $N_{SP}$. The durations of unsaturated flows are denoted by $T_{UV}$ and $T_{UP}$, with the mean number of passed vehicles and pedestrian platoons denoted by $N_{UV}$ and $N_{UP}$ · $T_{Vi}$, $T_P$, $T_{SV}$, $T_{SP}$, $T_{UV}$, and $T_{UP}$ are expressed in seconds. $N_{SV}$, $N_{SP}$, $N_{UV}$, and $N_{UP}$ are in passenger-car units (pcu).

Figure 2 shows the conflict mechanism between right turns and pedestrians. In China, right turns on red (RTORs) are allowed at most signalized intersections. Therefore, vehicles tend to take the lead in occupying the conflict zone with the assumption of a continuous queue

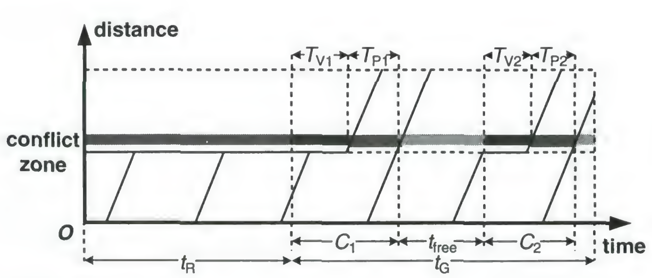


**FIGURE 2 Time–distance diagram of pedestrians conflicting with right turns.**

for vehicle capacity analysis. Pedestrians cross afterward. After that, there may be a period in which no pedestrians wait at the conflict zone until the next pedestrian platoon arrives. In Figure 2, $t_G$ is the effective green of the right turns in seconds, $t_R$ is the effective red in seconds, and $t_{free}$ is the time period in seconds when no pedestrians wait at the conflict zone during the effective green. During $t_G$, several conflict cycles may run at the conflict zone. For a specific conflict cycle *i*,

$$C_i = T_{Vi} + T_{Pi}$$

and

$$N_{Vi} = N_{SVi} + N_{UVi}$$

### Calculations for Saturated Vehicle Flow

When vehicles pass at the saturation flow rate, pedestrians are unable to cross and have to wait. The mean number of passed vehicles in the saturated flow usually accumulates during the period $T_P + T_{SV}$. Therefore,

$$N_{SV} = \frac{T_{SV} \cdot S_V}{3{,}600} = \frac{(T_P + T_{SV}) \cdot q_V}{3{,}600}$$

Then

$$T_{SV} = \frac{T_P \cdot q_V}{S_V - q_V} \tag{4}$$

where $S_V$ is the right-turn saturation flow and $q_V$ is the right-turn flow rate, both in passenger-car units per hour.

If RTORs are not allowed, the duration when the saturated vehicle flow accumulates should include the red phase interval $t_R$ (in seconds) in the first conflict cycle after the green indication is allocated. Therefore,

$$T_{SV} = \frac{(T_P + t_R) \cdot q_V}{S_V - q_V} \tag{5}$$

### Calculations for Unsaturated Vehicle Flow

When vehicles pass in unsaturated flow, pedestrians wait until the offered gap, *h* (in seconds), is larger than the pedestrian group critical gap, $t_{cP}$ (in seconds), and then occupy the conflict zone.

The probabilities that a certain number of vehicles will pass in the unsaturated flow are as follows:

One vehicle:

$$P_1 = P(h_1 < t_{cP}) \cdot P(h_2 > t_{cP})$$

Two vehicles:

$$P_2 = P(h_1 < t_{cP}) \cdot P(h_2 < t_{cP}) \cdot P(h_3 > t_{cP})$$

*n* vehicles:

$$P_n = P(h_1 < t_{cP}) \cdot P(h_2 < t_{cP}) \cdot \cdots \cdot P(h_n < t_{cP}) \cdot P(h_{n+1} > t_{cP})$$



Overtaking is usually forbidden in intersections; thus, the vehicle headways are shifted-exponentially distributed:

$$P(h \le t) = 1 - \exp\left[\frac{-q \cdot (t - t_m)}{(1 - q \cdot t_m)}\right] \tag{6}$$

where $t_m$ is the minimum follow-up time.

Suppose that

$$X_V = \exp\left[\frac{-q_V \cdot (t_{cP} - t_m)}{(1 - q_V \cdot t_m)}\right]$$

then

$$P(h > t_{cP}) = X_V$$

and

$$P(h \le t_{cP}) = 1 - X_V$$

Therefore,

$$P_n = (1 - X_V)^n \cdot X_V \tag{7}$$

The mean number of passed vehicles in the unsaturated flows can be calculated by using the following:

$$N_{UV} = \sum_{n=1}^{\infty} n \cdot P_n = \sum_{n=1}^{\infty} n \cdot (1 - X_V)^n \cdot X_V = \frac{1}{X_V} - 1 \tag{8}$$

When the offered gap is larger than $t_{cP}$, the right turns will be impeded. Thus, the headways in the unsaturated vehicle flows range from the minimum follow-up time $t_m$ to $t_{cP}$. The mean headway in the unsaturated flows can be calculated by using

$$H_{UV} = \frac{1}{q_V} - \frac{(t_{cP} - t_m) \cdot X_V}{1 - X_V} \tag{9}$$

The duration of the unsaturated vehicle flows can then be estimated as

$$T_{UV} = N_{UV} \cdot H_{UV} \tag{10}$$

### Estimates of Pedestrian Group Critical Gap

In most circumstances, when one waiting pedestrian accepts a gap, the others will follow to traverse the conflict zone. Therefore, the pedestrian group critical gap equals the minimum of the critical gaps of the individuals in the platoon.

The number of waiting pedestrians and the waiting time determine the critical gap of each individual. The critical gap of individual *j* in the waiting platoon is denoted by $t_{cPj}$ (in seconds), with the waiting time denoted by $d_j$ (in seconds); then

$$t_{cP} = \min_j (t_{cPj}) = \min_j \left[f(d_j, Q_P)\right] \tag{11}$$

where $Q_P$ is the number of waiting pedestrians.

If the pedestrians are assumed to be homogenous, the minimum critical gap of the individuals in the platoon is the critical gap of the individual who has waited for the longest period of time:

$$t_{cP} = f(d_j, Q_P) \tag{12}$$

where *d* is the waiting time of the pedestrian who has waited for the longest period of time in the platoon (in seconds).

$Q_P$ has been found to depend strongly on $d(r = 0.95)$, so the pedestrian group critical gap can be expressed as a function with regard to *d* only

$$t_{cP} = f(d, Q_P) = g(d) \tag{13}$$

As shown in Figure 2, *d* equals the time span in which the vehicle flow occupies the zone $T_{Vi}$.

When RTORs are not allowed, *d* should include the red phase interval in the first conflict cycle after the green indication is allocated:

$$d = \begin{cases} T_{V1} + t_R & \text{in first conflict cycle} \\ T_{Vi} & \text{in other conflict cycles } (i \ge 2) \end{cases} \tag{14}$$

### Calculations of Saturated Pedestrian Flow

On the basis of an analysis similar to that in the section on calculations of unsaturated vehicle flow, the time during which the pedestrians cross at the saturation flow rate can be estimated by using

$$T_{SP} = \frac{\left(\dfrac{l}{v_{P1}} + \dfrac{w_P^2 \cdot q_P}{v_{P1} \cdot l_s} \cdot d\right)}{\left(1 - \dfrac{w_P^2 \cdot q_P}{v_{P1} \cdot l_s}\right)} \tag{15}$$

where

$l$ = average width of conflicting vehicles (m),
$v_{P1}$ = mean speed of one-directional saturated pedestrian flow rate (m/s),
$w_P$ = mean diameter of pedestrians' bodies (m),
$q_P$ = average pedestrian arrival rate (ped/s), and
$l_s$ = effective crosswalk width (m).

### Calculations of Unsaturated Pedestrian Flow

Pedestrians in unsaturated flows are not delayed. Vehicles will impede the pedestrian flow when the offered gap, $h_P$, is larger than the vehicle critical gap, $t_{cV}$ (in seconds).

The probability that *n* pedestrian platoons will cross in the unsaturated pedestrian flow is

$$P_n = (1 - X_P)^n \cdot X_P \tag{16}$$

where $X_P = \exp\left(\dfrac{-(t_{cV} - 1)}{H_p - 1}\right)$.

The mean number of platoons that can pass during the unsaturated flow is

$$N_{UP} = \sum_{n=1}^{\infty} n \cdot P_n = \frac{1}{X_P} - 1 \tag{17}$$

The duration of the unsaturated pedestrian flow is then

$$T_{\mathrm{UP}} = N_{\mathrm{UP}} \cdot H_{\mathrm{UP}} \tag{18}$$

The vehicle critical gap should guarantee that vehicles can start up with no pedestrians in front.

Therefore,

$$t_{\mathrm{cV}} = \frac{t_{\mathrm{SL}} + l}{v_{\mathrm{UP}}} \tag{19}$$

where $t_{\mathrm{SL}}$ is the vehicle start-up time in seconds and $v_{\mathrm{UP}}$ is the mean speed of the unsaturated pedestrian flow in meters per second.

### Capacity of Conflict Zone During Conflicting Periods

The parameters $T_{\mathrm{SV}i}$, $T_{\mathrm{UV}i}$, $t_{\mathrm{cP}i}$, $N_{\mathrm{UV}i}$, $H_{\mathrm{UV}i}$, $T_{\mathrm{SP}i}$, and $d_i$ can be determined from a system composed of Equations 4, 8 through 10, and 13 through 15. The model reflects the fact that the conflict-zone capacity is determined by interactions between pedestrians and vehicles as well as by traffic characteristics.

The number of vehicles that can pass during the total conflicting period, $\Sigma_i C_i$, is

$$N_V = \sum_i N_{Vi} \tag{20}$$

## CAPACITY OF RIGHT-TURNING MOVEMENTS INFLUENCED BY PEDESTRIANS

### Considerations for Two-Way Pedestrian Traffic

The model describes conflicts between vehicles and one-way pedestrian flow. When the model is applied to two-way pedestrian traffic, the following adjustments are needed.

#### *Time Duration of Saturated Pedestrian Flow*

The mean flow speed strongly affects the duration of saturated pedestrian flow. Teknomo (*7*) concluded that the mean speed of two-way pedestrian flows is considerably lower than that of one-way flows. Therefore, $v_{\mathrm{P1}}$ as well as $q_P$ in Equation 15 should be replaced by values for two-way pedestrian flows.

#### *Pedestrian Platoon Headway Distribution*

When pedestrian platoons moving in two opposite directions are analyzed as a whole, the minimum pedestrian platoon headway is zero. Thus, the platoon headways are exponentially distributed as

$$P(h_p \le t) = 1 - \exp\left[\frac{-t}{(H_P - 1)}\right] \tag{21}$$

#### *Estimates of Pedestrian Group Critical Gap*

For a specific conflict zone, the pedestrians from the far curb often arrive later than those from the near curb. Therefore, pedestrians from the near curb tend to wait for a longer time and be more impatient. To simplify the analysis, it is assumed that the unsaturated vehicle flows are always impeded by pedestrians from the near curb. Then the pedestrian group critical gap can be calculated by using Equations 13 and 14.

### Capacity of Right-Turning Movements Influenced by Pedestrian Traffic

The capacity of right-turning movements influenced by pedestrians, in passenger-car units per hour, can be calculated by using

$$\mathrm{Cap} = \frac{3{,}600 \cdot (N_V + S_V \cdot T_{\mathrm{free}})}{C_{\mathrm{signal}}} \tag{22}$$

where $C_{\mathrm{signal}}$ is the cycle length of the intersection in seconds and $T_{\mathrm{free}}$ is the total time span in which no pedestrians are waiting at the conflict zone during the effective green of the right turns.

### Model Calibration

A total of 7 h of video was recorded at two typical signalized intersections in Beijing. The important characteristics of the two sites are given in Table 1.

The videotape yielded 321 pedestrian gap-acceptance processes. The observed accepted gaps have a mean of 5.1 s and a range of 8.2 s. Ashworth's method (*8*) was employed to estimate the pedestrian group critical gaps for various levels of *d*. Figure 3 shows the dependence between the pedestrian group critical gap and *d*. The regression model fitted to the data has an explanatory value of $r^2 = 0.71$.

Also obtained from the videotape were 52 pairs of $(N, p)$ data with 5-min intervals. The observed pedestrian volumes ranged from 290 to 1,380 ped/h, and the observed mean platoon sizes ranged from 1.59 to 3.23 ped. The data are a measure of pedestrian arrivals in platoons. The linear model was calibrated as follows:

$$N = 1.1374 + 0.0014 \cdot p \qquad r^2 = 0.90$$

TABLE 1 Characteristics of Data Collection Sites

| | Academy Southern Road and Zaojun Temple Road | Zhanlan Road and Chegongzhuang Street |
|---|---|---|
| Weather condition | Sunny or cloudy | Sunny |
| Area type | Non-CBD | Non-CBD |
| Approach observed | Southbound and Westbound | Westbound |
| Right-turn lane | 1 exclusive lane | 1 exclusive lane |
| Right-turn vehicular volume | Moderate | Low |
| Pedestrian volume | Moderate or low | Moderate |
| Bicycle volume | Low or moderate | Low |
| Cycle length (s) | 120–140 | 95–120 |
| Signal phase | 3 | 2 |
| Number of cycles used for calibration | 85 | 38 |



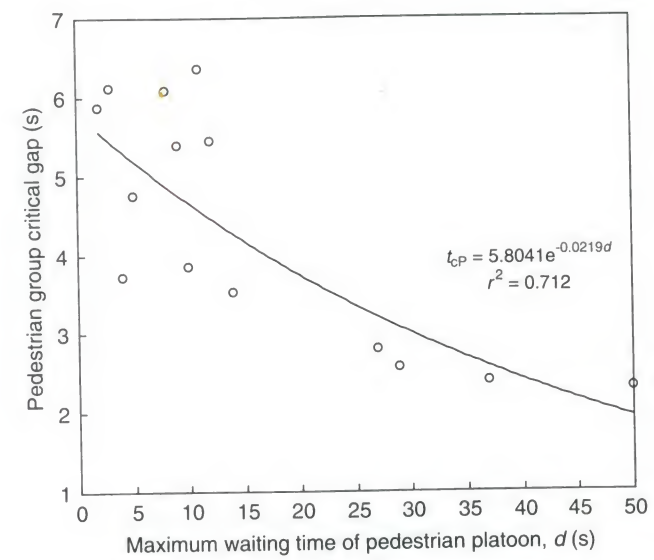


FIGURE 3 Relationship between pedestrian group critical gap and maximum waiting time of pedestrian platoon.

The other parameters were calibrated from the field observations as $t_m = 1.9$ s, $l_s = 5.1$ m, $l = 2.5$ m, $t_{\mathrm{cV}} = 2.5$ s, $v_{\mathrm{P2}} = 0.9$ m/s, and $w_{\mathrm{P}} = 0.6$ m. Because of the small sample of observations, these calibrated parameters are limited in scope and applicability.

## NUMERICAL EXAMPLE

### Inputs

The example will calculate the capacity of the northbound right-turning movement at the typical four-way intersection shown in Figure 1*a*. Each approach to the intersection has three lanes, a through lane, an exclusive left-turn lane, and an exclusive right-turn lane with ideal saturation flow rates of 1,800, 1,550 and 1,550 pcu/h, respectively. The lanes are 3 m wide with a zero-degree grade. The crosswalks are 4 m wide. The vehicle volumes of the through, left-turn, and right-turning movements are 500, 150, and 450 pcu/h, respectively.

Typical four-phase signal timing was used for the vehicles. The cycle length is 90 s, the amber indication is 2 s, and the all-red is 2 s, as is shown in Figure 4. The effective green is 27 s for the northbound right turns. RTORs are allowed. The right-of-way is allocated to pedestrians together with the through vehicle movements.

### Capacity Calculation and Results

In Phases 1 and 3, the northbound RTORs are not impeded by pedestrians, and the RTOR saturation flow rate was calculated on the basis of gaps in merging vehicle traffic. In Phase 2, the northbound right-turning movement conflicts with the pedestrians in the crosswalk on the northbound approach. In Phase 4, the movement conflicts with pedestrians in the crosswalk on the westbound approach. For various levels of the conflicting pedestrian volumes, the northbound right-turn capacities in Phases 2 and 4 were calculated by using the proposed model. Then the movement capacity was computed by summing the results for each phase.

The results indicate that pedestrians have a strong impact on the capacities at low conflicting pedestrian volumes and that the effects of additional pedestrians decrease as the pedestrian volumes increase, as is shown in Figure 5. The reason for the shape of the curves is that the number of pedestrian platoons rather than the pedestrian volume is used as the input for the gap-acceptance analysis. With the increase in volume, more pedestrians are included in each platoon. Therefore, the number of platoons increases less sharply as the volumes increase (Figure 6*a*). Accordingly, the average conflict times during the right-turn effective green also increase less sharply (Figure 6*b*). The capacities calculated by the model depend strongly on the average conflict times. Therefore, the results exhibit a logarithm-like relationship between the calculated capacities and the pedestrian volumes.

Another reasonable explanation, given by Rouphail and Eads (*4*), is that as the pedestrian volumes increase, they will tend to platoon more at the beginning of the cycle. The impact additional pedestrians have on vehicles is lessened because their path is already interfered with by the other pedestrians in the platoon.

In fact, the vehicle capacity of turning movements should depend strongly on the average conflict times during the vehicle effective green, because as the average conflict times increase,

- Pedestrians will occupy the conflict zone for longer times and
- More time is lost because of starting and braking of the vehicles.

The proposed model is able to describe this point, as is shown in Figure 7.

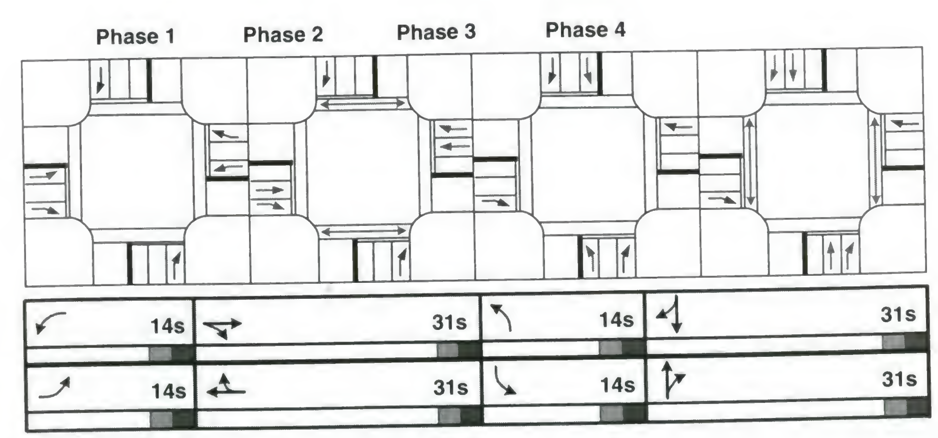


FIGURE 4 Signal timing scenario of example intersection.

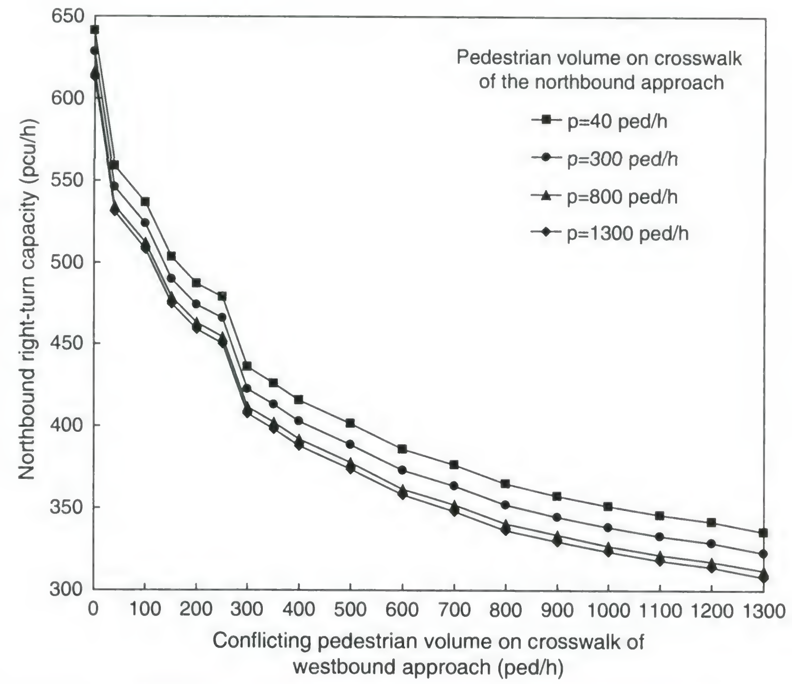


FIGURE 5 Sensitivity of right-turn vehicle capacity to conflicting pedestrian volume.

## SIMULATION EXPERIMENTS

VISSIM, a widely used microscopic simulation software, was employed in this study to validate the proposed model.

### Simulation Tests

VISSIM designates the right-of-way for conflicting movements by setting priority rules, which is the key step in modeling the interactions at the conflict zone. The capacity of right-turning movements influenced by pedestrians is simulated assuming no priority as the conflict mechanism (the conflicting vehicles and pedestrians wait for acceptable gaps in the competing flows and alternately get the right-of-way). The assumption is similar to that of the proposed analytical model.

In many places, vehicles are required to give way to pedestrians in the crosswalks, which is favorable for pedestrians but may not actually occur in many circumstances. In the simulation tests, the right-turn capacity in this pedestrian-friendly condition is also simulated by assuming that vehicles strictly yield to pedestrians.

At each pedestrian volume, 10 runs were made with the same 10 random number seeds. Each run time covered a period of 3,600 s. The input volume for the right-turn lane was 1,300 pcu/h, which will create a saturated condition in that lane.

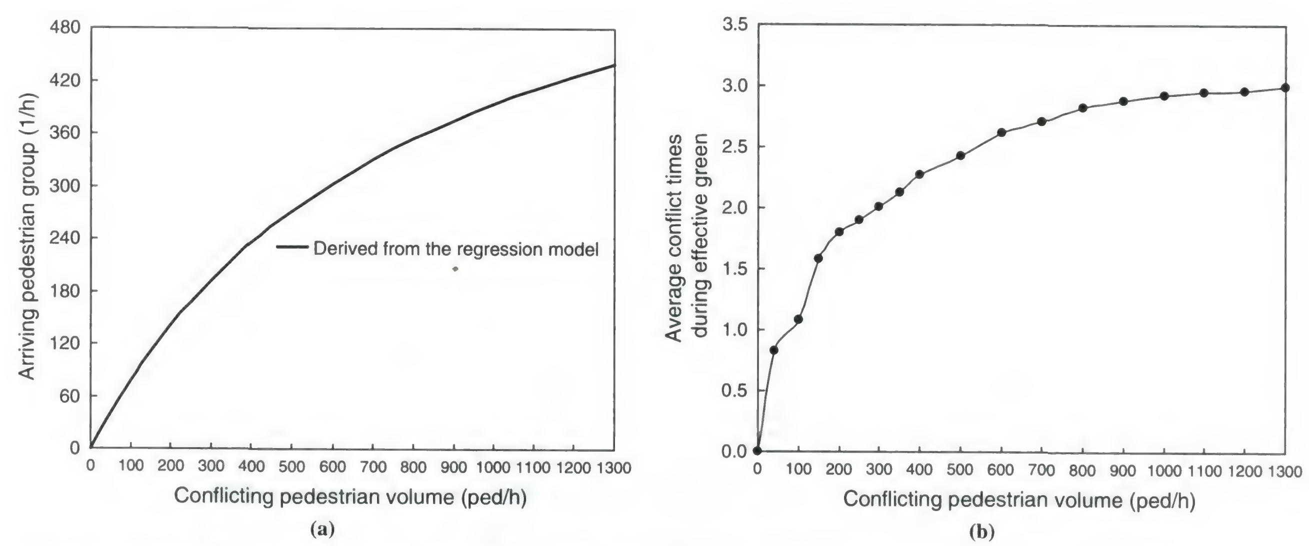


FIGURE 6 Sensitivity analyses for proposed model: (*a*) number of pedestrian platoons versus conflicting pedestrian volume and (*b*) average conflict times during effective green versus pedestrian volume.



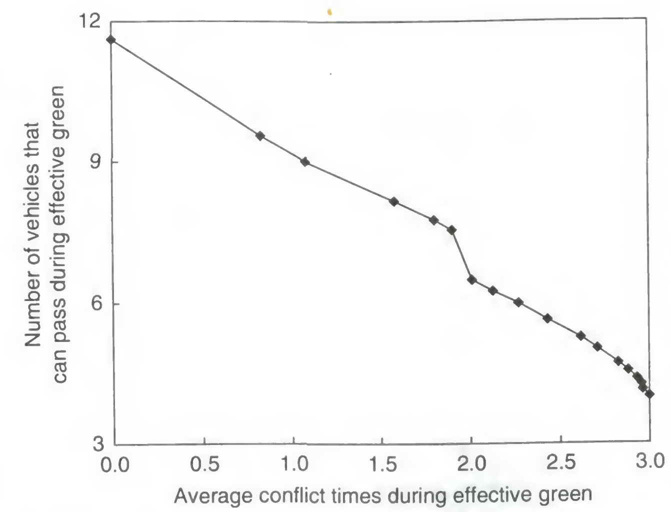


FIGURE 7 Sensitivity of number of vehicles passing during effective green versus average conflict time.

The parameters used for the simulations are the same as their counterparts in the proposed analytical model. The average of the simulated capacities was taken as the right-turn capacities for each pedestrian volume level.

### Analysis of Simulated Delay and Turning Speed

When vehicles are required to yield, the simulated vehicle delay caused by the pedestrians increases linearly as the conflicting pedestrian volume increases. With a no-priority assumption, the impact of additional pedestrians on simulated delay decreases as the pedestrian volume increases, as is shown in Figure 8*a*.

Different priority-rule assumptions resulted in small differences in the simulated turning speeds, as is shown in Figure 8*b*.

The simulated capacities correlate well with the right-turn speed. Figure 9 shows the relationships for various desired turning speed distributions (normal distributions), and Figure 10 indicates the effect of the desired turning speed distribution on the turning speed.

## COMPARISONS WITH ANALYTICAL MODELS AND SIMULATIONS

Two analytical models and two simulation models are compared with the proposed model. The capacity results are shown in Figure 11.

For the given conditions, the capacities yielded by various methods exhibit similar trends as the conflicting pedestrian volumes increase. The HCM (*1*) predicts the least effect of pedestrians on turning movement capacity. At low pedestrian volumes, the capacities by other methods all essentially agree, whereas at high pedestrian volumes, the results are influenced by the model assumptions for the priority rules.

The results yielded by the proposed model agree well with those by the VISSIM model, assuming no priority because of a similar assumption for the conflict mechanism. The assumption of pedestrian priority results in lower right-turn capacities. The results simulated by the VISSIM model with a pedestrian-priority assumption can be regarded as the lower bound of the right-turn capacities.

## CONCLUDING REMARKS

An analytical model was proposed to quantify the effect of pedestrians on right-turn capacity when pedestrians have no strict priority over vehicles. The model takes into consideration the pedestrian–vehicle conflict mechanism, pedestrian behavior, and their arrival

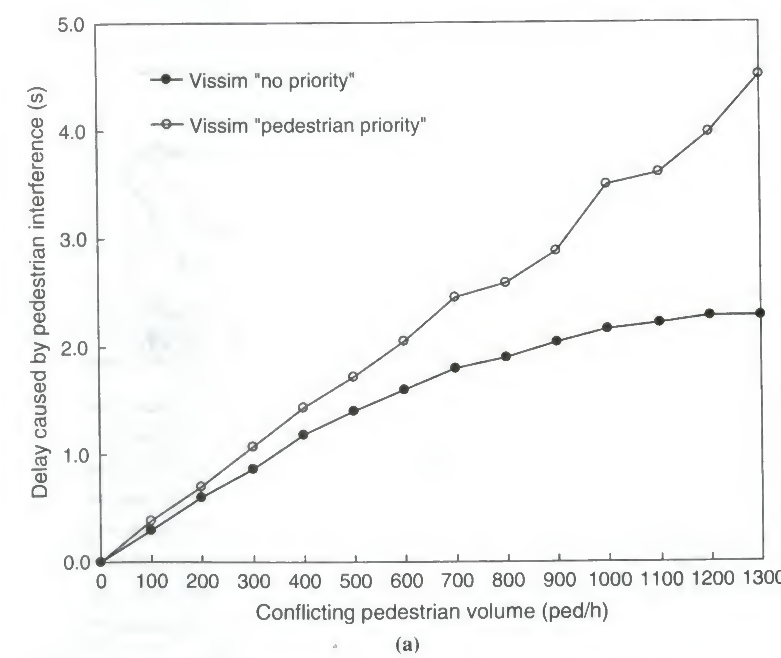


FIGURE 8 Effect of priority assumption on simulated vehicle flow characteristics: (*a*) sensitivity of right-turn vehicle delay caused by pedestrians to pedestrian volume.

(continued on next page)

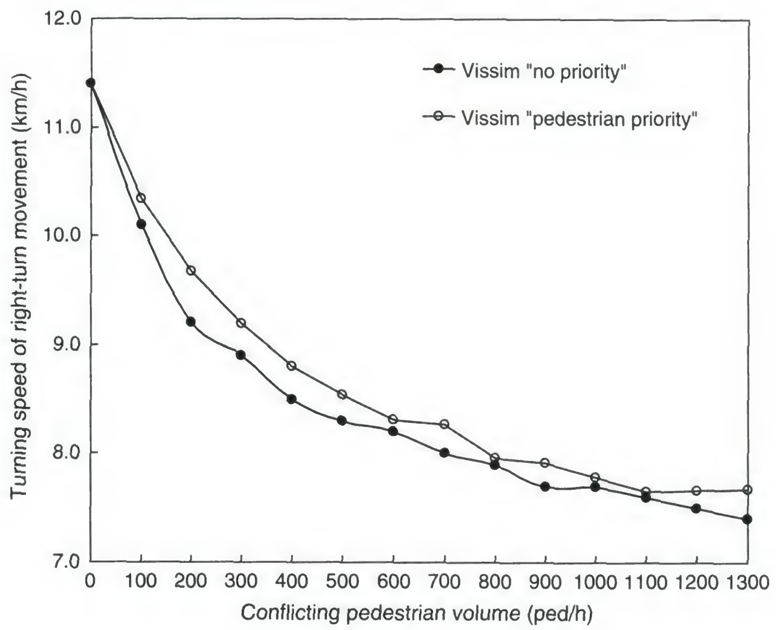

(b)

FIGURE 8 *(continued)* **Effect of priority assumption on simulated vehicle flow characteristics: *(b)* sensitivity of right-turn vehicle speed to pedestrian volume.**

in platoons. VISSIM was employed to validate the model, and comparisons with other models were made. The following conclusions can be drawn:

- The capacities calculated by the proposed model depend strongly on the average conflict times during the vehicle effective green. The capacities are generally lower than those yielded by the HCM and approximate those predicted by the VISSIM model with an assumption of no priority.
- Comparisons indicate that the HCM model predicts the least effect of pedestrians on turning movement capacities. At low pedestrian volumes, the results by the other methods agree reasonably well. At high pedestrian volumes, the models assuming pedestrian priority yield lower capacities than those assuming no priority.

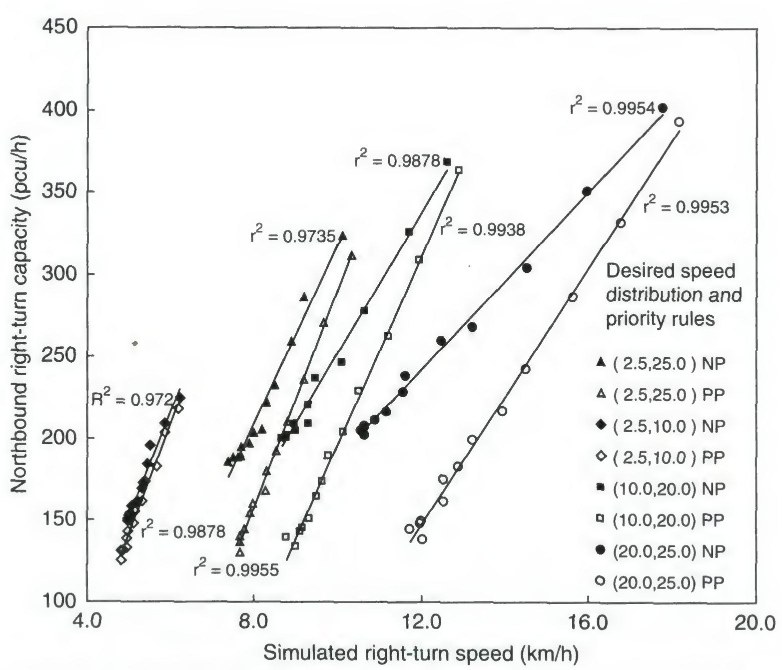


FIGURE 9 **Sensitivity of simulated right-turn vehicle capacity to turning speed (PP = pedestrian-priority assumption; NP = no-priority assumption).**



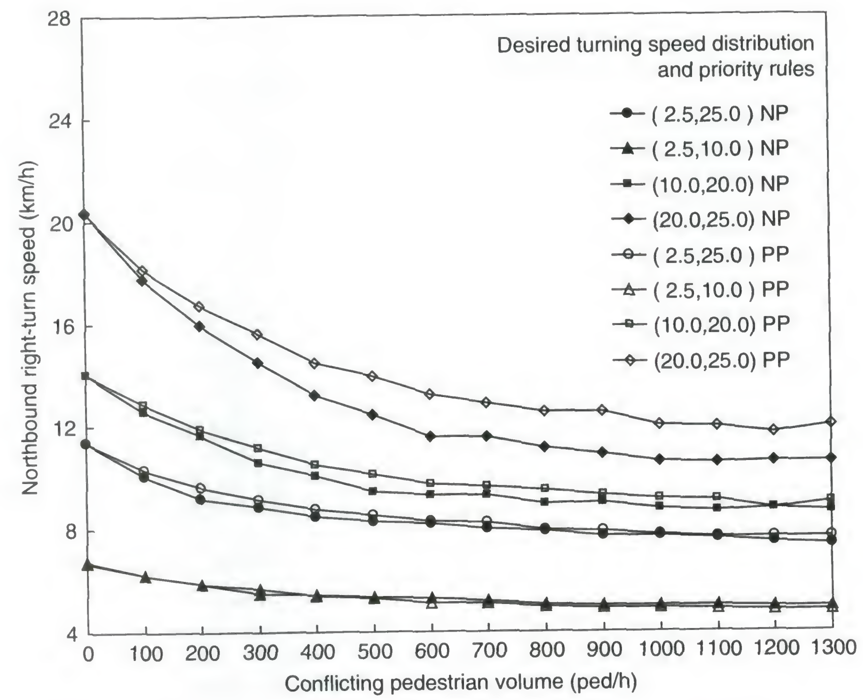


FIGURE 10 **Effect of desired turning speed distribution on mean turning speed.**

- The simulated capacities depend linearly on the turning speed of the right-turning movement. Different priority-rule assumptions result in small differences in the simulated turning speeds.
- Because of the small sample of observations, the calibrated model may be limited in scope and applicability. Subsequent work will focus on data collection at more intersections in various cities for calibration. Moreover, study of the influence of pedestrians on the capacity of left-turning movements at signalized intersections is in progress to provide a more complete capacity calculation methodology.

A gap-acceptance-based model to quantify the effect of bicycles on capacities of signalized intersections is provided elsewhere (*9*).

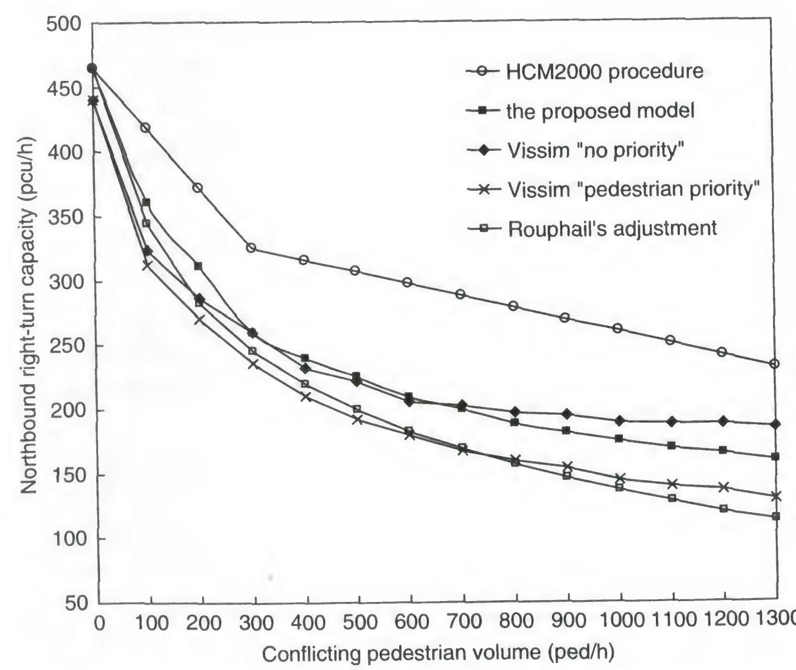


FIGURE 11 **Comparison of right-turn capacities yielded by various methods.**

## ACKNOWLEDGMENTS

This study constitutes one component of a pedestrian and bicycle project supported by the Key Technologies Research and Development Program of the Ministry of Science and Technology of China, the National Basic Research Program of China, and the Research Foundation of Beijing Jiaotong University.

## REFERENCES

1. *Highway Capacity Manual.* TRB, National Research Council, Washington, D.C., 2000.
2. Milazzo, J. S., II, N. M. Rouphail, J. E. Hummer, and D. P. Allen. Effect of Pedestrians on Capacity of Signalized Intersections. In *Transportation Research Record 1646,* TRB, National Research Council, Washington, D.C., 1998, pp. 37–46.
3. Allen, D. P., J. E. Hummer, N. M. Rouphail, and J. S. Milazzo II. Effect of Bicycles on Capacity of Signalized Intersections. In *Transportation Research Record 1646,* TRB, National Research Council, Washington, D.C., 1998, pp. 87–95.
4. Rouphail, N. M., and B. S. Eads. Pedestrian Impedance of Turning-Movement Saturation Flow Rates: Comparison of Simulation, Analytical, and Field Observations. In *Transportation Research Record 1578,* TRB, National Research Council, Washington, D.C., 1997, pp. 56–63.
5. Viney, N. D., and R. L. Pretty. Saturation Flow of a Movement Subject to a Pedestrian Stream at Traffic Signals. *Proc., 11th Conference of the Australian Road Research Board,* 1982, pp. 157–166.
6. Huang, W., and P. Yang. Delays of Pedestrians and Vehicles at Nonsignalized Zebra Crossing. *Journal of Tong-ji University,* Vol. 23, No. 1, 1995, pp. 31–36.
7. Teknomo, K. Application of Microscopic Pedestrian Simulation Model. *Transportation Research,* Vol. 9F, No. 1, 1995, pp. 15–27.
8. Brilon, W., R. Koenig, and R. J. Troutbeck. Useful Estimation Procedures for Critical Gaps. *Transportation Research,* Vol. 33A, No. 3–4, 1999, pp. 161–186.
9. Chen, X., C. Shao, and Y. Hao. Influence of Bicycle Traffic on Capacity of Typical Signalized Intersection. *Tsinghua Science and Technology,* Vol. 12, No. 2, 2007, pp. 198–203.

*The Pedestrians Committee sponsored publication of this paper.*

# Segway Rider Behavior

## Speed and Clearance Distance in Passing Sidewalk Objects

Sheryl Miller, John A. Molino, Jason F. Kennedy, Amanda K. Emo, and Ann Do

**The Segway Human Transporter is becoming more prevalent on urban sidewalks. This experiment investigated the approach speed and passing clearance that Segway devices exhibit on encountering a variety of obstacles on the sidewalk. The experiment was conducted with a sample of 20 Segway operators: 10 experienced operators and 10 novices. For the given experimental course and procedures, the results of the study revealed that (*a*) Segway riders approach obstacles at a mean speed of about 4.5 mph (7.2 km/h) with a range from 2.7 mph (4.3 km/h) to 6.8 mph (10.9 km/h); (*b*) Segway riders pass obstacles with a mean clearance of about 14.5 in. (36.7 cm) with a range from 3.3 in. (8.4 cm) to 43.2 in. (110 cm); (*c*) Segway riders pass moving pedestrians at an average speed of about 5 mph (8.1 km/h) and with an average clearance of 35.9 in. (91.2 cm); (*d*) Segway riders pass obstacles more slowly by about 0.5 mph (0.8 km/h) on average and closer by about 17.6 in. (44.7 cm) on average on a narrow as opposed to a wide sidewalk; and (*e*) experienced Segway riders pass faster by about 1.9 mph (3.1 km/h) on average than do novice riders. In the current experiment, the average passing event involving a Segway rider and a pedestrian required a minimum total distance of approximately 7.0 ft (2.1 m). These data should assist engineers in calculating the impact of various mixes of Segway traffic on sidewalks.**

The Segway Human Transporter is one of several low-speed transportation devices (e.g., bikes, scooters, wheelchairs) that, under certain circumstances, travel on sidewalks, roadways, and other shared-use paths. The Segway is a motorized device that can achieve a top speed of 12.5 mph (20.1 km/h). Segway users operate the device in a standing position, which allows the Segway to have a relatively small footprint. In order to accommodate Segway traffic, it is necessary to investigate riders' behavior under naturalistic sidewalk travel conditions.

## BACKGROUND

The Segway is marketed as a self-balancing transportation device that runs on battery power and uses a combination of gyroscopes, tilt sensors, and computer processors to stay balanced (*1*). One source has indicated that there are approximately 6,000 Segway devices in operation (*2*), but this number may be an underestimation because of the recent emergence of Segway tour companies around the country. However, there is little publicly available literature on the evaluation of Segway usability or safety. Instead, a small number of researchers have considered the Segway among a larger class of personal transportation devices such as motorized scooters, wheelchairs, and bicycles. At issue is how the Segway interacts with other users on shared-use paths and roadways.

Some non-FHWA literature has described the Segway in the context of benefits and costs to individual riders and society. Liu and Parthasarathy (*3*) provided an overview of the potential benefits of Segway ridership (e.g., pollution reduction) and potential challenges (e.g., the cost of the device). Litman and Blair (*4*) suggested features for characterizing different personal mobility devices, including the Segway. They characterized the Segway as having medium speed, medium size, and medium maneuverability when compared with other nonmotorized facility users such as individual walkers (e.g., low speed, high maneuverability) and human-powered bicycles (e.g., medium to large size, medium to low maneuverability).

Other researchers proposed empirical research on such devices, including the Segway. Shaheen and her colleagues (*5, 6*) introduced the concept of the Segway as a transportation connectivity device. They conducted a feasibility analysis and presented a plan for introducing low-speed modes of travel to users of California's Bay Area Rapid Transit (BART) system. Regarding safety, the authors concluded that among all the modes studied, the risk of injury in low-speed travel is slight. Although the Segway is part of the proposed BART pilot program, no crash or injury statistics from its use were included in the analysis.

In an FHWA-sponsored study, Landis and his colleagues provided one of the few research efforts to actually provide empirical analysis of Segway usage (*7, 8*). The researchers conducted an experimental field study of trail users, including bicycle riders, in-line skaters, people pushing strollers, wheelchair users, Segway riders, and others, who were videotaped as they rode through a defined course. The authors presented a comparative outline of pertinent operating statistics like physical dimensions of the device, turning radius, braking distance, and others. For example, for the Segway the mean speed was 9.5 mph (15.2 km/h), the mean perception–reaction time was 1.06 s, and the mean stopping distance was 8.8 ft (2.7 m). Unfortunately, these findings were not broken down by speed key. The speed key determines the maximum speed that the Segway can achieve: black key, 6 mph (9.7 km/h); yellow key, 8 mph (12.8 km/h), and red key, 12.5 mph (20.1 km/h). Navigation around obstacles was not evaluated, nor did the study involve novice Segway users.

S. Miller, J. A. Molino, and J. F. Kennedy, Science Applications International Corporation, Turner–Fairbank Highway Research Center, 6300 Georgetown Pike, F-215, McLean, VA 22101. A. K. Emo and A. Do, Federal Highway Administration, Turner–Fairbank Highway Research Center, 6300 Georgetown Pike, T-301, McLean, VA 22101. Corresponding author: J. A. Molino, John.A.Molino@saic.com.

*Transportation Research Record: Journal of the Transportation Research Board, No. 2073,* Transportation Research Board of the National Academies, Washington, D.C., 2008, pp. 125–132.
DOI: 10.3141/2073-14